A Mode Tracking Method for Flow Classification

Tianfeng Lu* and Mingjie Wang
Department of Mechanical Engineering
University of Connecticut, Storrs, CT 06269

Chun Sang Yoo and Jacqueline H. Chen
Combustion Research Facility
Sandia National Laboratories, Livermore, CA 94551

Chung K. Law
Department of Mechanical and Aerospace Engineering
Princeton University, Princeton, NJ 08544

Abstract
Chemical modes are independent kinetic processes in combustion systems obtained through computational singular perturbation (CSP), intrinsic low-dimensional manifold (ILDM), or simple eigen-decompositon. Transition of active chemical modes between explosive and non-explosive states plays a critical role in determining such limit phenomena as ignition and extinction, and in pinpointing flame front locations. It is shown in the present study that, by tracking the mode transition, a complex reacting flow may be classified locally as a plug flow reactor (PFR), stirred reactor (SR), and premixed or non-premixed flames. The mode tracking method is first demonstrated with 0-D reactors, including PFR and SR, and 1-D premixed and non-premixed flames. It is then applied to a turbulent lifted hydrogen jet flame in heated air coflow, computed with direct numerical simulation (DNS). The skeletal flame structure was visualized for the lifted flame, locally classified with mode tracking.

Introduction

Detailed chemical kinetic mechanisms typically involve a large number of chemical species and reactions, which are coupled with one another and may at the same time interact with transport processes. Such couplings frequently render chemically reacting flows difficult to analyze, under either laminar or turbulent conditions.

For flows that can be described by a finite set of nonlinear ordinary differential equations (ODEs), the governing equations may be decoupled through a mode analysis, with such methods as intrinsic low-dimensional manifold (ILDM) [1] and computational singular perturbation (CSP) [2, 3].

To obtain solutions with high order accuracy for nonlinear ODEs, the refinement procedure in CSP, based on the full Jacobian of the ODEs, can be employed to separate the fast modes from the slow ones [2, 3], such that the fast and slow subspaces are decoupled. Mode separation can also be achieved based on the chemical Jacobian, provided that the fast modes are dominated by fast chemical processes [1].

The methods of ILDM and CSP have been widely employed in such fields as mechanism reduction and stiffness removal, in which the fast chemical processes are assumed to be exhausted, such that they can be described by a set of algebraic equations [4-8].

For locally linearized systems, mode separation can be achieved through a simple eigen-decomposition, while concepts in CSP, such as the radical point [2, 3], may still be employed in quantifying the relations between the species and the independently evolving modes [9].

In addition to mechanism reduction, mode analysis is also an effective approach for flow analysis, where the controlling chemical processes can be identified from the complex flow fields through mode separation. For example, chemical explosive mode obtained with CSP has been applied in analyzing counterflow ignition [10] and the auto-ignition in flow reactors [11].

Recently, a method of explosive mode analysis (EMA), based on the Jacobian matrix of the chemical source term, was proposed and applied in several elementary combustion systems, including auto-ignition and premixed flames [12], as well as in the diagnostics of a turbulent lifted hydrogen jet flame into heated coflowing air, computed by direct numerical simulation (DNS) [13]. The role of auto-ignition in the stabilization of the lifted flame was suggested among several possible schemes investigated in previous studies, such as premixed and non-premixed flames [14-17], auto-ignition [18, 19], and

*Corresponding author: tlu@engr.uconn.edu
Proceedings of the 6th U.S. National Combustion Meeting

turbulence-flame interactions [16, 20, 21]. Furthermore, the locations of the lean premixed flame fronts were pinpointed using EMA.

In the present study, the method of mode tracking was developed based on an extended EMA for flow diagnostics. The mode tracking was first demonstrated in 0-D and 1-D diffusive systems to show the mode transitions occurring in typical combustion systems. It is then applied in the analysis of the lifted hydrogen flame simulated in Ref. [13] for further flow classification. The auto-igniting zones, premixed flame fronts, and non-premixed flames were subsequently identified and a skeletal flame structure was visualized.

Methodology

Chemical reaction is typically the driving force in combustion problems, characterized by rapid heat releases and radical proliferation. The evolvement of typical reacting flows can be represented by the following ODEs in the Lagrangian coordinate:

$$\frac{d\mathbf{y}}{dt} = \mathbf{g}(\mathbf{y}) = \boldsymbol{\omega}(\mathbf{y}) + \mathbf{s}(\mathbf{y}) \qquad (1)$$

where **y** is the vector of variables, such as species concentrations and temperature, **ω** is the chemical source term, and **s** includes all the non-chemical sources, such as diffusion and loss. The convective term is included on the LHS of eq. (1).

Applying the chain rule on eq. (1) and following a similar procedure as in CSP[2, 3], eq. (1) can be expressed in the form involving the Jacobians:

$$\frac{d\mathbf{g}}{dt} = \mathbf{J}\cdot\mathbf{g}(\mathbf{y}),\ \ \mathbf{J} = \frac{d\mathbf{g}}{d\mathbf{y}} = \mathbf{J}_\omega + \mathbf{J}_s,$$
$$\mathbf{J}_\omega = \frac{d\boldsymbol{\omega}}{d\mathbf{y}}, \text{ and } \mathbf{J}_s = \frac{d\mathbf{s}}{d\mathbf{y}}. \qquad (2)$$

Given a matrix of independent row vectors, **B**, eq. (2) can be further transformed to:

$$\frac{d\mathbf{f}}{dt} = \boldsymbol{\Lambda}\cdot\mathbf{f},\ \mathbf{f} = \mathbf{B}\cdot\mathbf{g},$$
$$\boldsymbol{\Lambda} = \frac{d\mathbf{B}}{dt}\cdot\mathbf{A} + \boldsymbol{\Lambda}_\omega + \boldsymbol{\Lambda}_s,\ \mathbf{A} = \mathbf{B}^{-1},$$
$$\boldsymbol{\Lambda}_\omega = \mathbf{B}\cdot\mathbf{J}_\omega\cdot\mathbf{A}, \text{ and } \boldsymbol{\Lambda}_s = \mathbf{B}\cdot\mathbf{J}_s\cdot\mathbf{A}, \qquad (3)$$

where **f** is the vector of mode. By choosing an appropriate vector set **B**, through, for example, the CSP refinement procedure[2], one may diagonalize or block-diagonalize matrix **Λ**, such that the modes can be decoupled. The application of CSP modes in combustion analysis has been extensively studied [22].

The term $(d\mathbf{B}/dt)\cdot\mathbf{A}$ in eq. (3) is nontrivial in general and indicates the rotation of the basis vectors. Numerical evaluation of such a rotation can be difficult particularly when the basis vectors are obtained through numerical iterations. However, for weakly nonlinear systems, such as in many combustion problems undergoing radical explosion or the post-ignition recombination stage, the time dependency of the chemical Jacobian $\mathbf{J}_\omega$ can frequently be neglected. In such cases, by choosing **B** to be the left eigenvectors of $\mathbf{J}_\omega$, $\boldsymbol{\Lambda}_\omega$ becomes a diagonal matrix, if a complete set of eigenvectors are available. The modes defined as such are named chemical modes in the following. Eq. (3) can then be transformed to:

$$\frac{df_i}{dt} = \lambda_i f_i\left[1 + \frac{1}{D_{a,i}}\left(\overline{\boldsymbol{\Lambda}}_{s,i}\cdot\bar{\mathbf{f}}_i\right)\right],\ i = 1, 2, ..., K,$$
$$D_{a,i} = \frac{\lambda_i}{\lambda_s},\ \overline{\boldsymbol{\Lambda}}_s = \frac{\boldsymbol{\Lambda}_s}{\lambda_s}, \text{ and } \bar{\mathbf{f}}_i = \frac{\mathbf{f}}{f_i} \qquad (4)$$

where λ_i is the *i*th eigenvalue of $\boldsymbol{\Lambda}_\omega$, which can be either positive or negative with the magnitude indicating the reciprocal time scale of the *i*th chemical mode, f_i. λ_s is the principal eigenvalue of $\boldsymbol{\Lambda}_s$, which is typically a negative number with the magnitude indicating the reciprocal time scale of the dissipation or loss processes. $D_{a,i}$ is the Damköhler number defined for the *i*th chemical mode, and $\boldsymbol{\Lambda}_{s,i}$ is the *i*th row of $\boldsymbol{\Lambda}_s$. *K* is the number of variables. By definition,

$$\overline{\boldsymbol{\Lambda}}_s = \mathbf{O}(1), \qquad (5a)$$

and for rate-controlling chemical modes:

$$\bar{\mathbf{f}}_i = \mathbf{O}(1). \qquad (5b)$$

If λ_i is a large negative value, and $|D_{a,i}| >> 1$, we have:

$$f_i \approx 0, \qquad (6)$$

which results in a low dimensional manifold described by the algebraic equation in eq. (6) [1].

On the other hand, if λ_i is a positive value, the associated chemical mode is a chemical explosive mode[12]. Furthermore, if $|D_{a,i}| >> 1$, the chemical explosive mode leads to explosion or ignition, since the system in eq. (4) is approximated as:

$$\frac{df_e}{dt} = \lambda_e f_e, \qquad (7)$$

where the subscript *e* indicates an explosive mode. Such a chemical explosive mode, f_e, is the driving force in many combustion systems. It is noted that, based on eq. (4), a chemical explosive mode may not always lead to explosion or ignition, if the time scale of the chemical explosive mode is not significantly shorter than that of the dissipation or loss processes. In such cases the chemical explosion may be suppressed by the loss.

Once a chemical explosive mode is obtained, the constituent variables, such as species and temperature, can be identified by the projection matrix:

$$\mathbf{Q}_e = \mathbf{a}_e\mathbf{b}_e, \qquad (7)$$

where $\mathbf{a}_e$ and $\mathbf{b}_e$ are the left and right eigenvectors, respectively, of the chemical explosive mode. The diagonal elements of $\mathbf{Q}_e$ indicate how strongly a species or temperature is related to the explosive mode [12].

The positive eigenvalue λ_e is a function of temperature, mixture composition, and chemical reactivity. Therefore it is a chemical property of the local mixture. Furthermore, chemical explosive modes evolve with the combustion processes, through which temperature and the mixture composition may change. As such, an chemical explosive mode may emerge or disappear during combustion. Such a transition process has been employed for classification of burned and unburned mixtures in premixed flames [12]. Such transition will further be shown to be important for flow classification in the present work.

Once the chemical explosive modes disappear, the entire system may consist of only decaying modes, which evolve to the equilibrium or steady states. An important task to track the change in an explosive mode is to identify which decaying mode it evolves to, immediately after the positive eigenvalue crosses zero.

It was shown in [12] that the Jacobian $\mathbf{J}_\omega$ is defective upon the positive eigenvalue crossing zero, when the eigenvector of the explosive mode rotates to that of a conservation mode. Therefore the mode composition defined in eq. (7) is not applicable at the crossover point, where matrix **B** is singular. In the present work, we assume that the λ_e at the crossover point is a continuous function of the chemical properties, including temperature and mixture composition. As such, the decaying chemical mode with the least negative eigenvalue is evolved from the chemical explosive mode after the crossover point. Once the explosive mode is linked to a decaying mode, the subsequent evolvement of the mode can be tracked by the mode composition, defined in eq. (7).

In the next section, such mode transitions in homogeneous and diffusive flows will be demonstrated.

Results and discussions

Mode tracking in 0-D reactors

Chemical explosive mode is important for auto-ignition, in which the loss term, **s**, is absent in eq. (1). Therefore with a positive eigenvalue λ_e, the system typically show a ignition behavior unless, in rare cases, the nonlinear effect of basis rotation in eq. (3) is sufficiently strong to skew the evolvement of the system. The chemical explosive mode and decaying mode evolved from it were tracked in the auto-ignition of a stoichiometric hydrogen-air mixture as shown in Fig. 1. The temperature profile is also plotted as a mark indicating the progress of the ignition. It is seen that the explosive mode, associated with a positive λ_e, exists prior to the ignition point, which is typically defined as the inflection point in the temperature curve. The explosive mode evolves quickly and becomes a decaying mode crossing the ignition point, after which the system consists of no explosive mode and is purely dissipative. It is further seen that the decaying mode evolved from the explosive mode features the slowest time scale in the system, as compared with the next slowest decaying mode associated with eigenvalue λ_2. There is no crossing between the two distinctive modes and therefore the chemical explosive mode can be unambiguously identified.

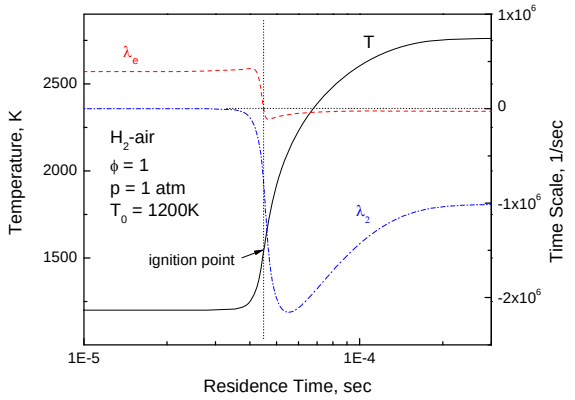

Figure 1. Evolvement of two least negative active chemical modes in auto-ignition of a stoichiometric hydrogen-air mixture.

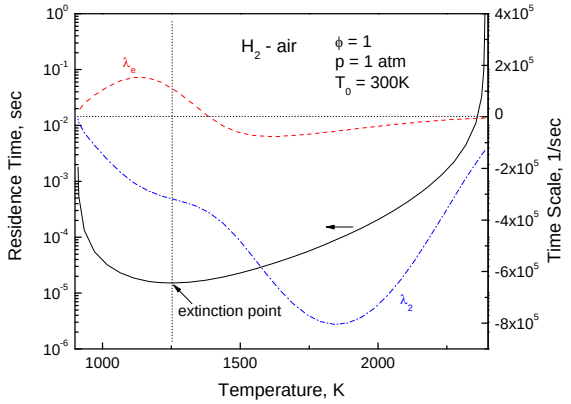

Figure 2. Evolvement of two least negative active chemical modes in a steady-state perfectly stirred reactor with stoichiometric hydrogen-air mixtures and inlet condition under STP.

While chemical explosive modes are typically the driving force of unsteady auto-igniting systems, it is also of importance in steady-state and extinction problems. Figure 2 shows the evolvement of a chemical explosive mode in a steady state perfectly stirred reactor (PSR). The profile for residence time vs. the reactor temperature consists of the transposed upper and middle branches of the combustion S-curve, with the extinction point being the turning point, or the local minima, in residence time.

It is seen that chemical explosive modes do not exist in the regime with high temperature and long residence time, where the reactants are mostly consumed and the system is near chemical equilibrium. With decreased residence time on the upper-branch, and consequently reduced temperature in the reactor, the amount of remaining reactants increases because of the reduced reactivity and limited residence time. When the system is sufficiently close to the extinction point, there is substantial amount of unconsumed reactants, such that the mixture becomes chemically explosive, as indicated by the emerging chemical explosive mode for temperature less than about 1500K. The formation of the turning point can consequently be explained with the chemical explosive mode:

Since the loss term of PSR features

$$\lambda_s = -\frac{1}{\tau}, \text{ and } \overline{\mathbf{\Lambda}}_s = \mathbf{I} \tag{8}$$

where τ is the residence time and $\mathbf{I}$ is the identity matrix, for weakly explosive mixtures with

$$\left|D_{a,e}\right| = \left|\frac{\lambda_e}{\lambda_s}\right| < 1, \tag{9}$$

the chemical explosive mode is suppressed by the loss and the mixture remains physically stable in steady state. With decreased residence time, the explosive mode becomes stronger and λ_e increases, such that at the turning point,

$$D_{a,e} = -1, \tag{10}$$

and the Jacobian $\mathbf{J}$ is singular, which is consistent with the mathematical definition of the turning point of steady state problems [23]. In the middle branch of the S-curve, as the chemical explosive mode becomes even faster,

$$\left|D_{a,e}\right| > 1, \tag{11}$$

such that there $\mathbf{J}$ features a positive eigenvalue and the system is physically unstable. Any small perturbation of the system will cause it to jump to either the upper- or the lower-branch of the S-curve. Therefore the singular Jacobian at the turning point in PSR is primarily induced by the change in the time scale of the chemical explosive mode.

It is further seen in Fig.2 that, similar to the observation in Fig. 1, the explosive mode can evolve and change to a non-explosive mode. While such a transition is not exactly the turning point, it is quite close to and strongly related to the turning. As such mode tracking is important in analyzing the extinction problem in PSR.

It is also observed from Figs. 1 and 2 that the mode transition in auto-ignition is abrupt, while that at extinction is more gradual. This is because the time scale of the chemical explosive mode is highly sensitive to temperature while there are abundant reactants in auto-ignition. In PSR, λ_e is most sensitive to the concentrations of the reactants, which varies gradually around the turning point. Therefore, the large activation energy effect of the H_2-air system is more clearly manifested in auto-ignition, resulting in the abruptness in the ignition curves in Fig. 1, while the changes are less abrupt in PSR.

Mode tracking in 1-D flames

To examine the mode tracking method in diffusive systems, we next apply it in a 1-D laminar premixed flame with a stoichiometric H_2-air mixture. Figure 3 shows the spatial profile of temperature as a marker for the flame structure. A chemical explosive mode and two decaying modes are also shown in the plot. It is seen that the chemical explosive mode exists in the preheat zone, where temperature is moderately high, say between about 800 and 1500K, and the mixture is unburned. In contrast to the auto-ignition in Fig. 1, λ_e in the premixed flame peaks near the edge of the preheat zone, next to the reaction zone. While the mixture is mostly non-explosive in the free-stream due to the low initial temperature (300K), the pre-mixture receives substantial heat and radicals from the reaction zone and rapidly becomes explosive. In such cases, the mixture may bypass the radical explosion stage and directly enter the stage of thermal run-away[12], which is an important feature of forced ignition.

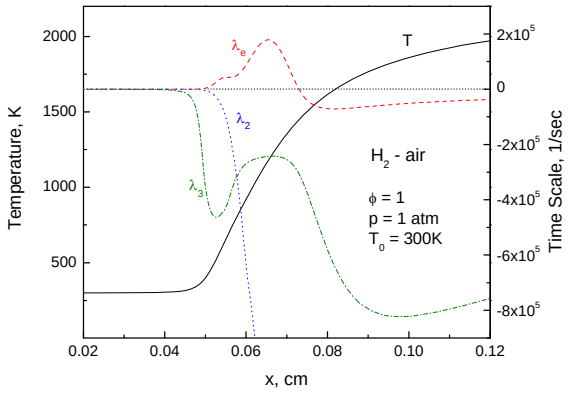

Figure 3. Mode tracking for a 1-D laminar premixed flame for stoichiometric H_2-air with free-stream mixture under STP.

Therefore, the transition of the explosive mixture to non-explosive mixture naturally defines the position of the premixed flame. This criterion was found to be effective in detecting partially premixed flame fronts in a lifted turbulent hydrogen jet flame simulated with DNS[13], that is difficult to analyze with many other criteria.

In addition to the chemical explosive mode, Fig. 3 further shows two decaying modes associated with the next two least negative non-zero eigenvalues, λ_2 and λ_3, respectively. An interesting observation is that the two

decaying modes cross each other. At the crossover point, the two modes are mixed because any linear combination of the two associated eigenvectors is still an eigenvector of the two modes. The mode crossing may also result in degenerated eigenvectors, which merits further study.

In non-premixed flames, chemical explosive mode does not necessarily exist. This point is demonstrated in Fig. 4, in which the least negative non-zero eigenvalue of $\mathbf{J}_\omega$ is shown to be negative across the entire flame. Near the peak of the temperature profile, where reactants are mostly consumed, the time scale of the chemical mode is short, indicating fast chemical reactions. In such cases D_a is a large positive number, and this property can be employed for detection of strongly burning non-premixed flames.

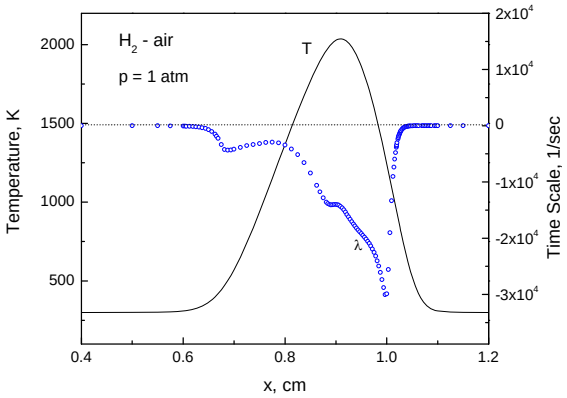

Figure 4. Spatial profiles of temperature and the least negative active chemical mode for a 1-D laminar non-premixed flame of opposed jets, with 50% of H_2 (in mole) diluted with N_2 on the left boundary (x = 0), and air on the right boundary (x = 2cm). Mixtures at both inlets are under STP with an inlet velocity of 100cm/s.

For non-premixed flames at near-extinction conditions, the flame temperature is sufficiently low and there may be substantial leakage of the reactants through the reaction zone. In such cases, chemical explosive mode may exist, and the flame becomes partially premixed.

Mode tracking and flow classification in a turbulent flame

EMA and mode tracking are further applied to analyze a 2-D snapshot from a 3-D DNS of a turbulent lifted hydrogen jet issuing into heated coflowing air. The lifted flame was simulated with a Sandia DNS code, S3D, which solves the compressible Navier-Stokes equations with detailed kinetics and transport. The inlet fuel jet consists of 65% hydrogen and 35% nitrogen by volume under atmospheric pressure, at a temperature of 400 K, and with a jet velocity of 347 m/s. The coflowing air is at 1100 K and has a velocity of 4 m/s. The jet Reynolds number is 11,000 based on the width of the slot, H, which is 1.92 mm. The size of the domain is 24 mm by 32 mm by 6.4 mm in the streamwise (x), transverse (y) and spanwise (z) directions, respectively. The simulation assumes nonreflecting inflow/outflow boundary conditions in the streamwise and transverse directions, and periodic boundary conditions in the spanwise direction. The snapshot was taken at 12 jet times, when the simulation has mostly reached the statistically steady state.

Due to the large number of grid points in the simulation, it is not feasible to solve the complete set of ODEs in eq. (1) obtained through numerical discretization, due to the time consuming eigen-decomposition for large equation sets. In the present study, the characteristic time scale of diffusion determined by λ_s is approximated by the local scalar dissipation rate [24].

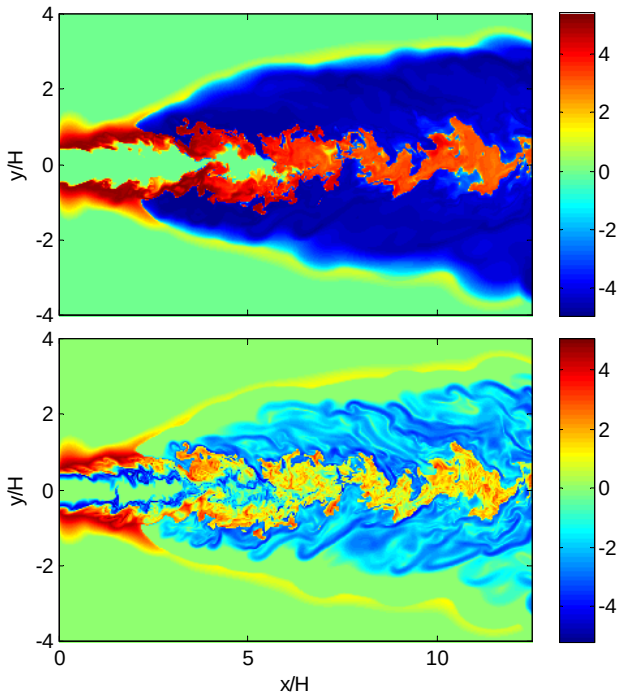

Figure 5. Isocontours of, (a) the time scale, $\pm log_{10}(|\lambda_1|$, 1/s), of the least negative active chemical mode and (b) the Damköhler number, $\pm log_{10}(|D_a|)$, in a lifted H_2 jet coflowing into heated air. Time scales longer than 1s were truncated to 1s for both the explosive mode and the scalar dissipation rate.

It is seen in Fig. 5a that strong chemical explosive mode (dark red) exists in the mixing layer near the nozzle exit, which is located at the center on the left boundary. The mixtures are non-explosive near the jet center close to the nozzle exit or deep into the coflowing air, where there is a lack of either oxygen or fuel, respectively. Downstream in the mixing layer, a region in blue colors consists of reactive but non-explosive, or burned mixtures, as discussed in detailed in[12]. The fork-shaped

sharp boundary separating the non-explosive (blue) and explosive (red/yellow) mixtures was identified as the partially premixed flame fronts, with the lean front on the air side and the rich front near the jet center. The leading position of the fork-shaped front was identified as the stabilization point of the lifted flame.

Fig. 5b shows the plot of Damköhler number defined with the least negative active chemical mode and the local scalar dissipation rate. Based on eq. (4), if the least negative mode is rate-controlling for the local mixture, the local flows can be roughly classified by the following categories:

Auto-igniting zone:

$$D_a = -O(1/\varepsilon) \tag{12a}$$

Non-premixed flames, or stirred reactors:

$$D_a = +O(1/\varepsilon) \tag{12b}$$

Premixed flames, or self-igniting fronts:

$$D_a \text{ crosses zero} \tag{12c}$$

It is noted that for non-premixed flames, the time scale of chemical reactions is significantly shorter than that of diffusion, such that the flame is diffusion-controlled. The strongly burning non-premixed flame zone therefore is on the upper-branch of the typical combustion S-curve, similar to strongly reacting stirred reactors.

Based on the above classification, the structure of the lifted flame is visualized in Fig. 6, and superimposed to the isocontour of temperature. It can first be seen that the red line encloses highly explosive mixtures, leads directly to the stabilization point, indicating that auto-ignition is the dominating factor causing the first (left most) blob of ignited mixtures in the flow field. The evolution of the mixtures enclosed in the red lines can be approximated by a plug flow reactor, or auto-ignition, for which diffusion is neglected.

Second, the forked-shaped premixed flame fronts (white lines) are stabilized by the ignited spot. The propagation of the premixed flame front to both the lean and the rich directions can be readily observed by following a flow particle downstream from the stabilization point. It is noted that the lean flame front is difficult to observe on the temperature plot, since temperature change is small across the lean flame where the concentration of H_2 is extremely low.

Third, the non-premixed flame zones, enclosed by the blue lines, largely overlap with the high-temperature zones in the mixing layer, which consists of highly-reactive but non-explosive post-ignition mixtures. The non-premixed flame is diffusion-controlled, with the fast chemical mode following the mixing processes.

While the flow structure identified above can facilitate the understanding of the flame stabilization mechanism and locating the flame surfaces, it can also be utilized to develop such simplified flow models as the reactor network model [25], which merits further investigation.

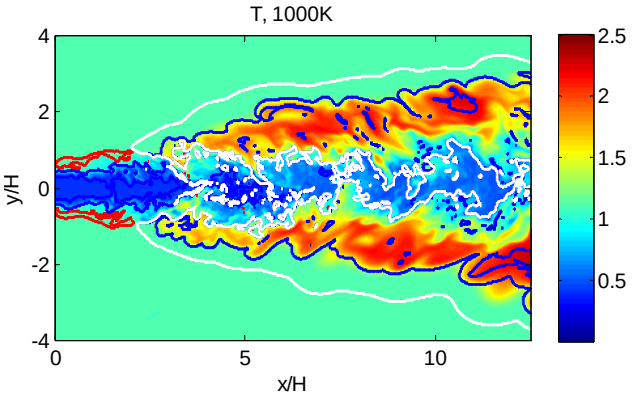

Figure 6 Different zones in the lifted hydrogen jet flame obtained by EMA and mode tracking, superimposed onto the temperature isocontour. Red line: isocontour of D_a = -10^4, Blue lines: D_a = +10, While lines: λ_e = 0.

Conclusions

The method of mode tracking was developed and EMA extended for flow diagnostics and classification. By tracking the transition of a chemical mode from explosive to non-explosive state, the rate-controlling chemical processes were identified for typical 0-D reactors and 1-D flames. Such information was then employed in the classification of local flows. A specific example of the lifted hydrogen jet into heated air simulated by DNS was employed to demonstrate the method. It was shown that chemical explosive mode is the driving force not only for many unsteady auto-igniting systems, but also for steady state extinction problems, e.g. the emergence of chemical explosive mode was found to be a primary factor in forming the extinction turning point in the S-curves in PSR.

A Damköhler number was defined based on the time scale of the controlling chemical mode and that of the dissipation or loss processes. The Damköhler number combined with the time scale of the associated chemical mode provides important information for flow classification. Auto-igniting zones, premixed and non-premixed flames can consequently be distinguished.

Compared to the classical CSP theory based on the full Jacobian matrix, the present method utilizes the Jacobian matrix of the chemical source term and is therefore simple to implement, even for many complex flow fields. While conclusive information can be obtained for cases with large Damköhler numbers (either positive or negative), the method may only provide limited guidance for cases with a Damköhler close to unity, i.e, when the chemical time scales are comparable to the flow time. Methods for flow classification that are applicable under such conditions are still to be explored.

Acknowledgements
The work at UConn and Princeton was supported by the Air Force Office of Scientific Research under the technical monitoring of Dr. Julian M. Tishkoff.

The work at Sandia National Laboratories (SNL) was supported by the Division of Chemical Sciences, Geosciences, and Biosciences, Office of Basic Energy Sciences of the U. S. Department of Energy, and the U. S. Department of Energy SciDAC Program. SNL is a multiprogram laboratory operated by Sandia Corporation, a Lockheed Martin Company, for the U. S. Department of Energy under contract DE-AC04-94AL85000. The simulation used resources of the National Center for Computational Sciences (NCCS) at ORNL, which is supported by the Office of Science of the U.S. DOE under contract DE-AC05-00OR22725.

References

1. U. Maas, and S.B. Pope, *Combustion and Flame,* 88 (1992), 239-264.
2. S.H. Lam, *Combustion Science and Technology,* 89 (1993), 375-404.
3. S.H. Lam, and D.A. Goussis, *International Journal of Chemical Kinetics,* 26 (1994), 461-486.
4. Z. Ren, and S.B. Pope, *Combustion and Flame,* 147 (2006), 243-261.
5. M. Valorani, F. Creta, D.A. Goussis, J.C. Lee, and H.N. Najm, *Combustion and Flame,* 146 (2006), 29-51.
6. T.F. Lu, and C.K. Law, *Combustion and Flame* (2008), in press.
7. S.H. Lam, "Singular perturbation for stiff equations using numerical methods", in *Recent advances in the aerospace sciences*, ed. by Corrado Casci in honor of Luigi Crocco, New York and London: Plenum Press, 1985.
8. T.F. Lu, C.K. Law, C.S. Yoo, and J.H. Chen, *Combustion and Flame* (in press).
9. T.F. Lu, Y.G. Ju, and C.K. Law, *Combustion and Flame,* 126 (2001), 1445-1455.
10. C.G. Fotache, T.G. Kreutz, and C.K. Law, *Combustion and Flame,* 108 (1997), 442-470.
11. A. Kazakov, M. Chaos, Z.W. Zhao, and F.L. Dryer, *Journal of Physical Chemistry A,* 110 (2006), 7003-7009.
12. T.F. Lu, C.K. Law, C.S. Yoo, and J.H. Chen, 'Analysis of a turbulent lifted hydrogen/air jet flame from direct numerical simulation with computational singular perturbation', Paper# AIAA-2008-1013, in *46th AIAA Aerospace Sciences Meeting and Exhibit,* Reno, Nevada, 2008,.
13. C.S. Yoo, R. Sankaran, and J.H. Chen, *Journal of Fluid Mechanics* (2008), submitted.
14. N. Peters, and F.A. Williams, *Aiaa Journal,* 21 (1983), 423-429.
15. A. Upatnieks, J.F. Driscoll, C.C. Rasmussen, and S.L. Ceccio, *Combustion and Flame,* 138 (2004), 259-272.
16. A. Joedicke, N. Peters, and M. Mansour, *Proceedings of the Combustion Institute,* 30 (2005), 901-909.
17. S.H. Chung, *Proceedings of the Combustion Institute,* 31 (2007), 877-892.
18. R. Cabra, T. Myhrvold, J.Y. Chen, R.W. Dibble, A.N. Karpetis, and R.S. Barlow, *Proceedings of the Combustion Institute*, 29 (2002), 1881-1888.
19. C.N. Markides, and E. Mastorakos, *Proceedings of the Combustion Institute,* 30 (2005), 883-891.
20. M.M. Tacke, D. Geyer, E.P. Hassel, and J. Janicka, *Proceedings of the Combustion Institute,* 27 (1998), 1157-1165.
21. L.K. Su, O.S. Sun, and M.G. Mungal, *Combustion and Flame,* 144 (2006), 494-512.
22. T.F. Lu, and C.K. Law, *Progress in Energy and Combustion Science* 35 (2009), 192-215.
23. S. Kalamatianos, Y.K. Park, and D.G. Vlachos, *Combustion and Flame,* 112 (1998), 45-61.
24. R.W. Bilger, *Proceedings of the Combustion Institute,* 22 (1988), 475-488.
25. M. Falcitelli, L. Tognotti, and S. Pasini, *Combustion Science and Technology,* 174 (2002), 27-42.